Calorimetric study of the smectic-A–smectic-C^* transition and the nematic–smectic-A–smectic-C^* point

Xin Wen and C. W. Garland
Department of Chemistry and Center for Material Science and Engineering, Massachusetts Institute of Technology, Cambridge, Massachusetts 02139

M. D. Wand
Displaytech, Inc., 2200 Central Avenue, Boulder, Colorado 80301

(Received 11 May 1990)

The phase behavior near the nematic–smectic-A–smectic-C^* (N–Sm-A–Sm-C^*) point has been studied with a high-resolution ac calorimetry technique in seven binary mixtures of two chiral compounds. The smectic-A (Sm-A)—smectic-C^*(Sm-C^*) phase transitions are continuous for all the mixtures studied. The Sm-A–Sm-C^* specific-heat variations are well described by the extended Landau model, with the possible exception of the mixture closest to the N–Sm-A–Sm-C^* composition. As the N–Sm-A—Sm-C^* point is approached, the Sm-A—Sm-C^* transition became more tricritical-like, indicating that the tricritical point (TCP) is located at or very near the N–Sm-A–Sm-C^* point. These observations contradict a previous report that the Sm-A–Sm-C^* TCP is displaced from the N–Sm-A–Sm-C^* point in this system. Anomalous C_p variations in the N range suggest a restructuring that might be associated with biaxial nematic fluctuations.

I. INTRODUCTION

The properties of the nematic–smectic-A–smectic-C (N–Sm-A–Sm-C) point are currently of great experimental[1–6] and theoretical[7–12] interest. The two most important unresolved questions about the N–Sm-A–Sm-C point are as follows. First, is the N–Sm-A—Sm-C point a Lifshitz point or a tetracritical point adjacent to an additional biaxial N' phase? Second, is the tricritical point (TCP) on the Sm-A–Sm-C transition line always located very near to or even precisely at the N–Sm-A–Sm-C point? If so, what are the physical reasons behind this?

The first question arises from the different predictions of two types of theoretical models for the N–Sm-A–Sm-C point. The first type of theory, originally developed by Chen and Lubensky (CL),[7] is based on a single (infinite-dimensional) order parameter for the smectic density and predicts that the N–Sm-A–Sm-C point is a Lifshitz point at which the transverse wave vector of the order parameter vanishes. This prediction was found to be in general agreement with the observations in a high-resolution x-ray scattering experiment.[1] The second type of theory[8–11] includes two order parameters, one for the smectic density modulation and one for the tilt angle of the direction in the Sm-C phase. Within this approach, Grinstein and Toner[8] (GT) have shown in a dislocation-loop melting theory that the N–Sm-A–Sm-C point should be a tetracritical point at which an additional biaxial N' phase should exist between the N and C phases. When fluctuations were included, it was found[2] that the CL model also produced the same type of phase diagram as the GT model. However, the N' phase and associated N–Sm-A–Sm-C–N' tetracritical point and NN' transition have not yet been observed in experiments.[3–6]

The second question related to the N–Sm-A–Sm-C point is the location of the TCP on the Sm-A–Sm-C transition line. Experimentally, a first-order N–Sm-C transition and a second-order Sm-A–Sm-C transition have been observed with the TCP being approached in both cases as the N–Sm-A–Sm-C composition is approached.[4–6,11,13] These previous observations suggest that the TCP for the Sm-A–Sm-C transition is very near to or perhaps at the N–Sm-A–Sm-C point.[11] In a recent Letter,[14] Parmar *et al.* presented a phase diagram for a binary mixture of two chiral compounds: 4-[(2R,3R)-expoxyhexyloxylphenyl-4-[(3S,7)-dimethyloctyloxybenzoate) (MDW74), and 4′[(s)-(4-methylhexyl)oxyl-phenyl-4-(decyloxy)-benzoate (W82). For this system they report that the TCP lies on the Sm-A–Sm-C^* line, displaced a considerable distance from the N–Sm-A–Sm-C^* point, and that the N–Sm-A transition is first order. The possibility of such a displaced TCP is supported by recent observations of first-order Sm-A–Sm-C^* phase transitions in materials with large spontaneous polarizations.[13,15–17]

The motivation of this high-resolution ac calorimetric study is first to determine quantitatively the location of the TCP on the Sm-A–Sm-C^* line in the MDW74-W82 system. A second aspect of the work is to characterize the N–Sm-A and N–Sm-C^* transitions near the N–Sm-A–Sm-C^* point, where different phase behaviors have been predicted by the two current types of theories.[7,8] Specific-heat measurements have been made on pure W82 and seven mixtures with MDW74 compositions ranging from 2 to 32 wt. %. The N–Sm-A–Sm-C^* point was found to be at $X_{\mathrm{MDW74}} \sim 19\%$. After subtraction of an appropriate background heat capacity, the excess heat capacity ΔC_p associated with the Sm-A–Sm-C^* transition is found to be well described by the usual "extended" Landau model.[3–6] Furthermore, as the N–Sm-A–Sm-

C^* point is approached, the heat capacity peak associated with the Sm-A–Sm-C^* transition shows an approach to a TCP. Thus the TCP is in the immediate vicinity of the N–Sm-A–Sm-C^* point, as observed in nonchiral systems. For $X_{\mathrm{MDW74}} \geq 6$ wt. %, the N–Sm-A transition is second order, in contrast to the proposed first-order N–Sm-A character reported previously.[14] The N–Sm-C^* phase transitions beyond the N–Sm-A–Sm-C^* point are clearly first order, as expected. A broad and rounded heat-capacity hump has been observed in the nematic phase at compositions close to the tricritical value, which may indicate the possible existence of biaxial fluctuations.

II. METHOD AND RESULTS

The high-resolution ac calorimetry technique used in this study has been described previously.[18,19] The sample cell, prepared in the same manner as in Ref. 17, consists of a silver cup and silver foil lid that is tightly wrapped over the lid of the cup. The total mass of the sample cell plus liquid crystal and addenda is about 0.5 g, of which 40–50 mg is the W82-MDW72 mixture.

The Sm-A–Sm-C^* transition temperature was found to decrease slowly with time, and this rate of T_c drift increases somewhat as the MDW72 composition increases to that of the N–Sm-A–Sm-C^* point. However, the largest drift rate observed for any of the mixtures was slower than -10 mK/day, and the temperature difference between Sm-A–Sm-C^* and N–Sm-A transitions was unchanged during a given experiment (several days). The scan rate near the Sm-A–Sm-C^* transition was about 100 mK/h, and the data reported in this paper were acquired during the first cooling run on a sample. The transition temperatures measured in this study, shown in Fig. 1, are consistent with previous results[14] within the resolutions of the respective experimental techniques.

Figure 2 shows the heat-capacity variations for seven different mixtures. The phase shift φ between the oscillating heat input power and the sample's T_{ac} temperature response provides useful qualitative information about the order of the phase transitions.[18,19] In Fig. 3 we show the phase shifts associated with N–Sm-A, Sm-A–Sm-C^*, and N–Sm-C^* transitions for several mixtures. The dip in the phase shift observed at the Sm-A–Sm-C^* transition is characteristic of a second-order phase transition, whereas the distinct peak in φ observed at the N–Sm-C^* transition is expected for first-order transitions. The data in Figs. 2 and 3 show that the N–Sm-A–Sm-C^* point corresponds to a X_{MDW74} value between 18 and 20 wt. %, in contrast to the value of $\sim$26 wt. % previously reported.[14] This discrepancy is not surprising in view of the relatively low resolution of the differential thermal analysis technique used in Ref. 14.

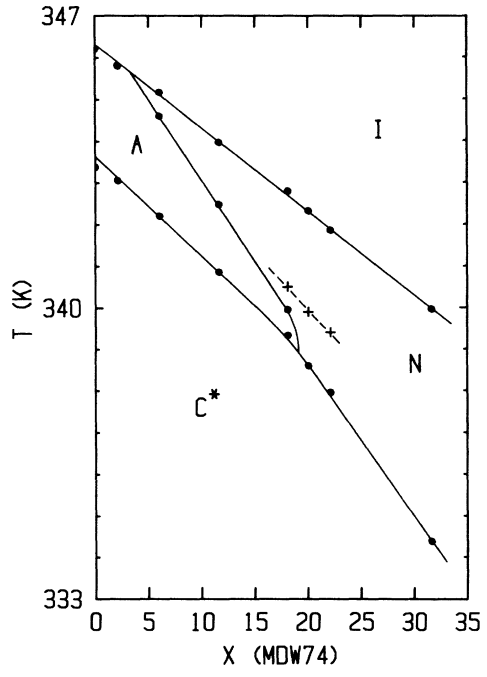

FIG. 1. Partial phase diagram for mixtures of MDW74 and W82. The circles are phase-transition points obtained in this study, and the solid lines are aids to the eye. The estimated locations of anomalous C_p behavior in the nematic phase are indicated by the plus signs (see text). X is the weight percent of MDW74.

III. DATA ANALYSIS AND DISCUSSION

Since the Sm-A–Sm-C^*, N–Sm-A, and I-N transitions are quite close to each other in temperature, all of the transitions contribute to the heat capacity near the temperature of the Sm-A–Sm-C^* transition. In order to analyze the excess heat capacity associated with the Sm-A–Sm-C^* transition, it was necessary to subtract the background contribution due to I-N and N–Sm-A (or I–Sm-A) peaks at higher temperatures:

$$\Delta C_p = C_p(\mathrm{obs}) - C_p(\mathrm{background}) \, . \tag{1}$$

The estimated background curves, which were obtained from a polynomial fit to the low-temperature wing of the N–Sm-A or I–Sm-A peak, are shown in Fig. 2. Since the N–Sm-C^* transition for the 20.03-wt. % mixture is very weakly first order, it is also of interest to look at the pretransitional $\Delta C_p(N$–Sm-$C^*)$ for this sample as was done in a previous N–Sm-A–Sm-C experiment.[3] The choice of C_p (background) is very difficult for the 18.09- and 20.03-wt. % samples. In Figs. 2(e) and 2(f), we show two choices—(a) the dashed curve is the same as C_p (background) chosen for the 6.04-wt. % sample shifted in temperature, and (b) the solid curve is our somewhat arbitrary estimate of the lowest feasible choice of C_p (background).

The resulting excess heat-capacity curves associated with the Sm-A–Sm-C^* transition are shown in Fig. 4. Just above the transition temperature, there is a very small non-Landau excess ΔC_p(Sm-A–Sm-C^*) tail, which

has often been observed for Sm-A-Sm-C transitions.[17,19] It may be due to either inhomogeneities or very weak pretransitional fluctuations.[17]

The usual "extended" Landau model was used to describe the Sm-A-Sm-C^* excess heat-capacity data and the N-Sm-C^* pretransitional ΔC_p for the 20.03-wt. % sample. In this model, the free-energy density G of the Sm-C^* phase is expressed as a power expansion of the Sm-C^* tilt order parameter ψ as follows:

$$G = G_0 + at\psi^2 + b\psi^4 + c\psi^6 , \tag{2}$$

where G_0 is the free-energy density of the Sm-A phase. The reduced temperature t is defined as $(T - T_0)/T_0$. The coefficients a and c are positive. Positive and negative values of b correspond to second- and first-order

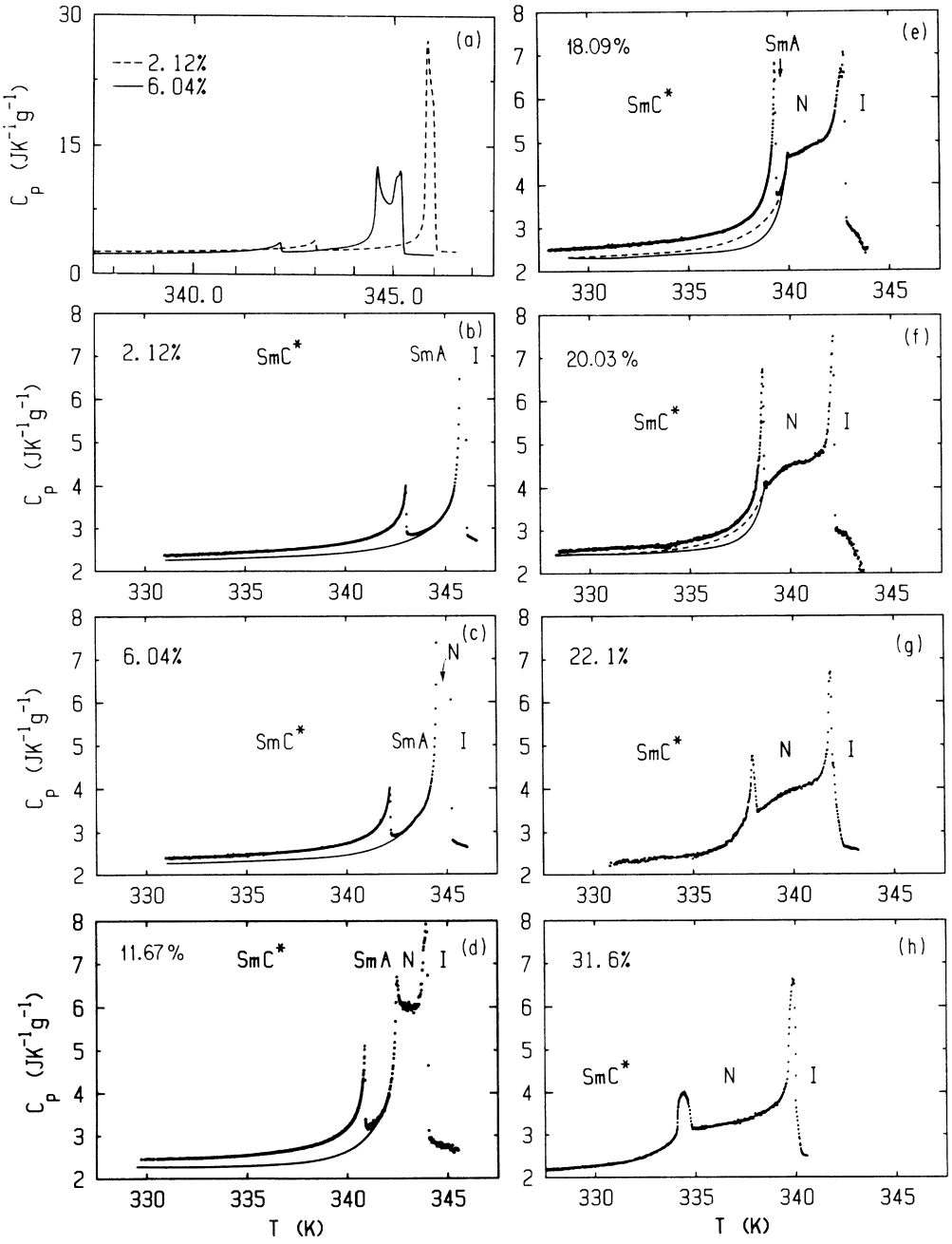

FIG. 2. Heat-capacity variations in W82+MDW74 samples containing 2.12, 6.04, 11.67, 18.09, 20.03, 22.1, and 31.6 wt. % of MDW74. The lines are the estimates for the background heat capacity in the vicinity of the Sm-A-Sm-C^* (or N-Sm-C^*) transition (see text). The first panel shows an expanded view of the 2.12- and 6.04-wt. % of data to illustrate the evolution of the Sm-A-I to Sm-A-N-I peak structure.

transitions, respectively; $b=0$ represents a tricritical point. The excess heat capacity below the transition temperature in this model is given by

$$\Delta C_p=(AT/T_0^{3/2})(T_k-T)^{-1/2}, \quad (3)$$

with $A=(a^3/12c)^{1/2}$ and $T_k=T_0+(b^2/3ac)T_0$. ΔC_p vanishes for $T>T_0$ for a second-order transition, and for $T>T_1=T_0+(b^2/4ac)T_0$ for a first-order transition.

Using the expression in Eq. (3), good fits with χ^2 around 1 were obtained over a 10-K temperature range for pure W82 and the three mixtures with $X=2.12$, 6.04, and 11.67 wt. %. In the case of the 18.09- and 20.02-wt. % samples, good Landau fits could be obtained with the low C_p (background), choice (b) represented by the solid lines in Figs. 2(e) and 2(f), but not with the dashed C_p (background), choice (a). The Landau fits for Sm-A–Sm-C^* transitions are shown in Fig. 4, and the pa-

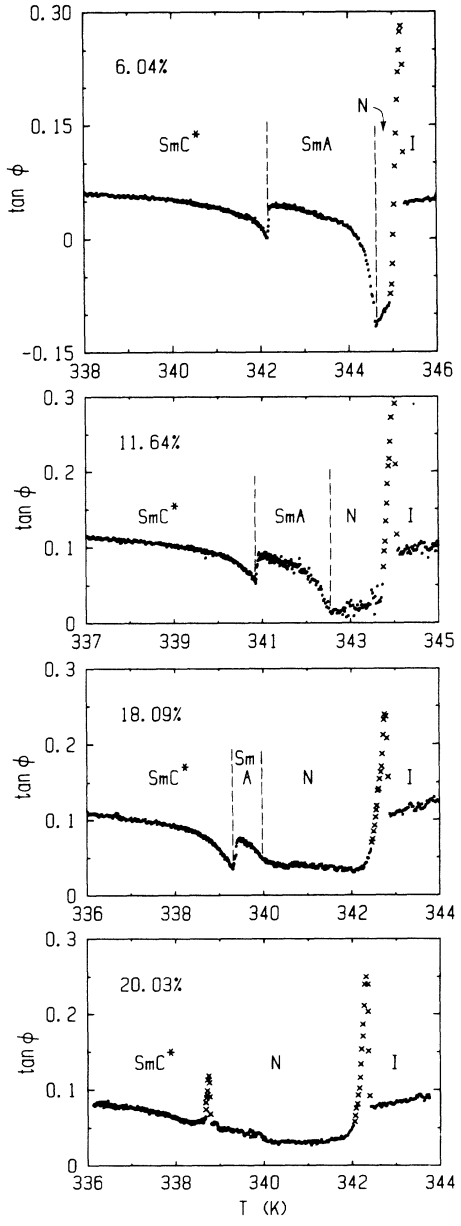

FIG. 3. Phase shift φ between the oscillating heater power and the sample response temperature for $X_{\mathrm{MDW74}}=6.04$, 11.64, 18.09, and 20.03 wt. %. Positions of N–Sm-A and Sm-A–Sm-C^* transitions, as determined by peaks in C_p, are indicated by vertical dashed lines. Points indicated by a cross (×) represent two-phase coexistence at a first-order transition.

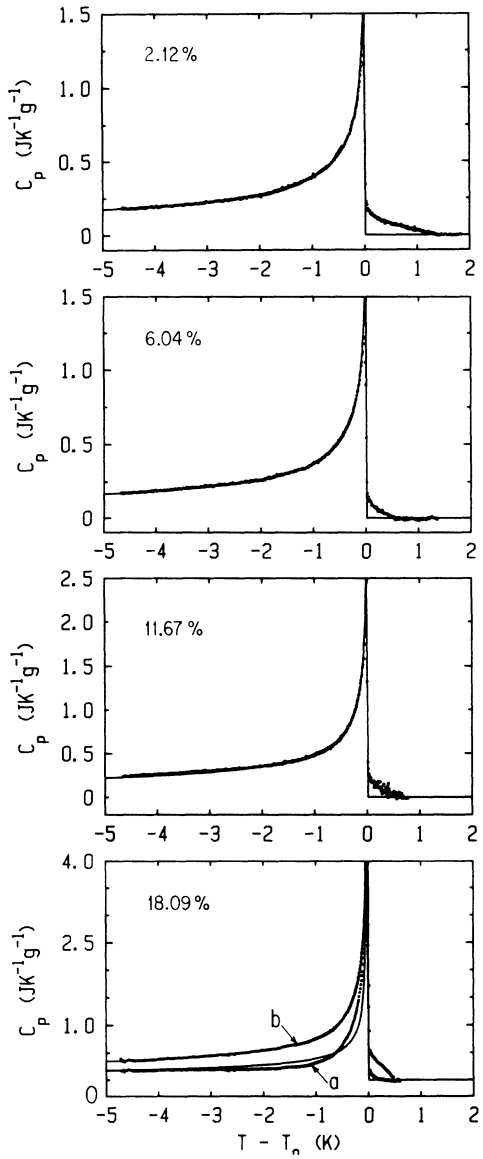

FIG. 4. Excess heat-capacity variations for samples with 2.12, 6.04, 11.67, and 18.09 wt. % MDW74 and the Landau fitting curves. The fits were obtained over the range $-10<(T-T_0)<0$ K using Eq. (3), but only part of that range is displayed here. The quality of the fit is good all the way out to -10 K, but ΔC_p becomes quite sensitive to the choice of C_p (background) far from T_0. For the 18.09-wt. % sample, two ΔC_p variations and their respective fits are shown: (a) ΔC_p based on choice (a) for C_p (background), which is the dashed line in Fig. 2(e); (b) ΔC_p based on choice (b) for C_p (background), which is the solid line in Fig. 2(e).

TABLE I. Results of least-squares fits of the excess heat-capacity variation near Sm-A-Sm-C^* transitions (N-Sm-C^* for 20.03 wt. %) using the expression in Eq. (3). δH is the integrated transition enthalpy $\int \Delta C_p dT$. T_{max} and T_{mid} are the temperatures at the maximum and the half height (on the high-temperature side) of the ΔC_p(Sm-A-Sm-C^*) or ΔC_p(N-Sm-C^*) peak.

X_{MDW74} (wt. %)	T_{max} (K)	T_{mid} (K)	T_k (K)	$T_k - T_{mid}$ (mK)	A (J g^{-1})	χ^2	δH_{total} (J g^{-1})
0	343.31	343.370	343.430	60	7.55	1.28	2.43
2.12	343.03	343.055	343.110	55	7.44	0.70	2.36
6.04	342.16	342.190	342.234	44	7.09	0.86	2.41
11.67	340.87	340.880	340.909	29	9.29	1.03	3.10
18.09[a]	339.326	339.370	339.337		7.22	47.0	3.71
18.09[b]	339.326	339.370	339.359		14.30	0.80	4.90
20.03[a]	338.625	338.680	338.564		5.05	32.9	(2.00)[c]
20.03[b]	338.625	338.680	338.617		9.53	0.85	(2.12)[c]

[a] C_p(background) choice (a): the dashed curve in Fig. 2.
[b] C_p(background) choice (b): the solid curve in Fig. 2.
[c] This $\delta H_{N\text{-Sm-}C^*}$ value does not include any latent heat contribution.

rameter values are given in Table I. The transition temperature T_0 has been somewhat arbitrarily taken to be T_{mid}, the midpoint of the rapid drop on the high-temperature side from the maximum observed C_p value to the background, as having been done for all other Sm-A-Sm-C transitions.[19–22] This choice has no effect on the shape of ΔC_p; it only determines the temperature at which the theoretical ΔC_p drops to zero. For $X_{MDW74} = 18.09\%$, $T_k - T_{mid}$ is slightly negative, which has also been seen in previous Sm-A-Sm-C^* work.[17] A possible reason for this effect is the rounding of the large heat-capacity peak near a TCP because of small composition inhomogeneities.

The good description of the Sm-A-Sm-C^* transition with the extended Landau model is consistent with previous observations.[4–6,19–22] A breakdown of this Landau description very close to the N-Sm-A-Sm-C^* point has been reported by Anisimov *et al.*[4,5] Such non-Landau behavior occurs here for the choice (a) background heat-capacity curve (see Fig. 4 and Table I). However, it is possible to obtain Landau behavior for ΔC_p with the choice (b) background. The difficulty in establishing an unambiguous background near the N-Sm-A-Sm-C^* point makes resolution of this question uncertain. The N-Sm-A-Sm-C^* region is further complicated by an anomalous C_p behavior in the N phase, as described below. In any event, the increase in the integrated enthalpy $\delta H = \int \Delta C_p dT$ as the N-Sm-A-Sm-C^* point is approached (see Table I), and the decrease in $(T_k - T_0) \cong (T_k - T_{mid})$ along the Sm-A-Sm-C^* line, indicate that the TCP for the Sm-A-Sm-C^* transition is near the N-Sm-A-Sm-C^* point. This finding is consistent with observations made on nonchiral N-Sm-A-Sm-C systems.[3–6,11]

In contrast to the continuous Sm-A-Sm-C^* transitions, the N-Sm-C^* transitions observed for $X > X_{N\text{-Sm-}A\text{-Sm-}C^*} \cong 19$ wt. % MDW74 are clearly first order, as illustrated in Figs. 2 and 3. These observations further support the idea that the TCP is in the immediate vicinity of the N-Sm-A-Sm-C point.

It should be noted in Fig. 2 that a broad, rounded heat-capacity "hump" exists in the nematic region for samples with $X = 18\%$, 20%, and 22%. This hump suggests that a substantial restructuring occurs within the N phase on cooling. If confirmed by further experiments,[23] this might provide experimental evidence of biaxial or cholesteric modulation in the N phase. The estimated locations of these anomalous nematic humps are shown on the phase diagram in Fig. 1. A careful examination of the C_p behavior reported by Anisimov *et al.*[4] suggests that similar anomalies may occur near the N-Sm-A-Sm-C point in $\overline{6}08 + \overline{6}010$ mixtures (see, in particular, Fig. 6 of Ref. 4); however, the data are too limited to draw any firm conclusions about that system.

As shown by the ac phase-shift data in Fig. 3, the N-Sm-A transitions appeared to be second order for $X_{MDW74} \geq 6\%$. In all likelihood, the N-Sm-A transition becomes first order at lower X. This would be expected on the basis of the narrow temperature range of the nematic phase in that region.[24]

IV. CONCLUSION

We have reexamined the phase diagram for binary chiral mixtures of W82 and MDW74 with a high-resolution ac calorimetry technique. The TCP on the Sm-A-Sm-C^* transition line has been found to be very close to the N-Sm-A-Sm-C^* point, rather than away from the N-Sm-A-Sm-C^* point as proposed in Ref. 14. Furthermore, the N-Sm-A transition appeared to be continuous in the vicinity of the N-Sm-A-Sm-C^* point, instead of first order as proposed in Ref. 14.

The observation of a broad heat-capacity hump in the N region for samples with X_{MDW74} near the N-Sm-A-Sm-C composition provides evidence of substantial restructuring in the N phase. This very interesting possibility is worth further investigation.

ACKNOWLEDGMENTS

We would like to thank Dr. G. Nounesis for his valuable help with the experimental technique and for stimulating discussions. This project was supported in part by the National Science Foundation through Grant No. DMR87-19217. Synthesis of the MDW74 sample was supported by U.S. Air Force Grant No. F3315-87-C-5293.

[1]L. J. Martinez-Miranda, A.R. Kortan, and R. J. Birgeneau, Phys. Rev. Lett. **56**, 2264 (1986); Phys. Rev. A **36**, 2372 (1987).

[2]L. Solomon and J. D. Litster, Phys. Rev. Lett. **56**, 2268 (1986).

[3]C. W. Garland and M. E. Huster, Phys. Rev. A **35**, 2365 (1987).

[4]M. A. Anisimov, V. P. Voronov, A. O. Kulkov, V. N. Petukhov, and F. Kholmurodov, J. Phys. (Paris) **46**, 2137 (1985).

[5]M. A. Anisimov, V. P. Voronov, A. O. Kulkov, V. N. Petukhov, and F. Kholmurodov, Mol. Cryst. Liq. Cryst. **150**, 399 (1987).

[6]J. Thoen and R. Parret, Liq. Cryst. **5**, 479 (1989).

[7]J. C. Chen and T. C. Lubensky, Phys. Rev. A **14**, 1202 (1976).

[8]G. Gristein and J. Toner, Phys. Rev. Lett. **51**, 2386 (1983).

[9]K. C. Chu and W. L. McMillan, Phys. Rev. A **15**, 1181 (1977).

[10]L. Benguigui, J. Phys. (Paris) Colloq. **40**, C3-419 (1979).

[11]C. C. Huang and S. C. Lien, Phys. Rev. Lett. **47**, 1917 (1981).

[12]G. Gristein, T. C. Lubensky, and J. Toner, Phys. Rev. B **33**, 3306 (1986); T. C. Lubensky (private communication).

[13]H. Y. Liu, C. C. Huang, C. Bahr, and G. Heppke, Phys. Rev. Lett. **61**, 345 (1988).

[14]D. S. Parmar, N. A. Clark, D. M. Walba, and M. D. Wand, Phys. Rev. Lett. **62**, 2136 (1989).

[15]C. Bahr and G. Heppke, Mol. Cryst. Liq. Cryst. Lett. **4**, 31 (1986).

[16]B. R. Ratna, R. Shashidhar, G. G. Nair, S. K. Prasad, C. Bahr, and G. Heppke, Phys. Rev. A **37**, 1824 (1988).

[17]J. Boerio-Goates, C. W. Garland, and R. Shashidhar, Phys. Rev. A **41**, 3192 (1990).

[18]C. W. Garland, Thermochim. Acta **88**, 127 (1985).

[19]M. Meichle and C. W. Garland, Phys. Rev. A **27**, 2624 (1983).

[20]C. R. Safinya, M. Kaplan, J. Als-Nielsen, R. J. Birgeneau, D. Davidov, and J. D. Litster, Phys. Rev. B **21**, 4199 (1980); R. J. Birgeneau, C. W. Garland, A. R. Kortan, J. D. Litster, M. Meichle, B. M. Ocko, C. Rosenblatt, L. J. Yu, and J. Goodby, Phys. Rev. A **27**, 1251 (1983).

[21]C. C. Huang and J. M. Viner, Phys. Rev. A **25**, 3385 (1982).

[22]C. C. Huang and S. Dumrongrattana, Phys. Rev. A **34**, 5020 (1986).

[23]A conoscopic test for biaxility was attempted in the N phase near the N–Sm-A–Sm-C point, but this was not successful because of of strong streaks presumably caused by cholesteric twisting of the director.

[24]M. E. Huster, K. J. Stine, and C. W. Garland, Phys. Rev. A **36**, 2364 (1987).